High-Performance Photocatalytic Degradation of Methylene Blue Dye by NiO-Integrated Bentonite/Fe_3O_4

Fahma Riyanti[1,*], Hasanudin[2], Addy Rachmat[2], Muharni[2], Eddy Ibrahim[3], and Poedji Loekitowati Hariani[2,*]

[1]Doctoral Program of Mathematics and Natural Sciences, Faculty of Mathematics and Natural Sciences, Universitas Sriwijaya, Ogan Ilir, Indonesia
[2]Department of Chemistry, Faculty of Mathematics and Natural Sciences, Universitas Sriwijaya, Ogan Ilir, Indonesia
[3]Department of Mining Engineering, Faculty of Engineering, Universitas Sriwijaya, Ogan Ilir, Indonesia
Email: fatechafj@unsri.ac.id (F.R.); hasanudin@mipa.unsri.ac.id (H.); addy_rachmat@unsri.ac.id (A.R.); muharnimyd@yahoo.co.id (M.); eddyibrahim@ft.unsri.ac.id (E.I.); puji_lukitowati@mipa.unsri.ac.id (P.L.H.)
*Corresponding author
Manuscript received February 6, 2025; revised March 19, 2025; accepted April 30, 2025; published August 5, 2025

***Abstract*—Environmental pollution from wastewater containing dyes has emerged as a significant issue, necessitating research to identify effective catalysts to address this problem. The present study investigation generated a bentonite/Fe_3O_4@NiO composite as a photocatalyst for the degradation of Methylene blue dye. The composite was examined utilizing X-Ray Diffraction (XRD), Scanning Electron Microscope with Energy-Dispersive X-ray Spectroscopy (SEM-EDX), UV-vis Diffuse Reflectance Spectroscopy (UV-DRS), Vibrating Sample Magnetometer (VSM), and Fourier Transform Infrared Spectroscopy (FTIR). The bentonite/Fe_3O_4@NiO composite exhibits magnetic properties by a saturation magnetization value of 51.02 emu/g. With a low band gap of 1.96 eV, this composite is active in the visible light region. NiO supported on bentonite/Fe_3O_4 enhances degrading efficiency relative to bentonite/Fe_3O_4. The degradation efficiency attained 99.35% under visible light irradiation with optimal conditions: 0.05 g of catalyst, 20 mg/L Methylene blue dye concentration, pH 8, and an irradiation time of 75 min. The photocatalytic degradation adhered to the pseudo-first-order model. The bentonite/Fe_3O_4@NiO composite exhibited remarkable stability, with an efficiency reduction of merely 5.71% after five reuse cycles. This photocatalyst could potentially be utilized in the remediation of wastewater-containing dyes.**

***Keywords*—Bentonite/Fe_3O_4@NiO composite, photocatalyst, degradation, visible light, methylene blue dye**

I. Introduction

Synthetic dyes, such as Methylene blue dye, are extensively utilized across multiple industries, including textiles, paper, pharmaceuticals, leather, and cosmetics [1, 2]. Annually, the textile industry utilizes more than 80,000 metric tons of reactive coloring agents; nonetheless, 20-30% of these chemicals are discarded as they are not absorbed by the fabric [3]. The environmental and health repercussions of dye-induced water contamination are significant. Dyes are challenging to break down naturally due to their intricate and stable chemical composition. Consequently, these dyes can persist in water for extended periods, diminishing the sunlight penetration essential for photosynthetic organisms. The disposal of dye-containing waste into the environment might result in significant pollution [4, 5].

Methylene blue dye ($C_{16}H_{18}ClN_3S$) is a basic dye that is regularly utilized and known for its stability and capacity to produce brilliant hues. Methylene blue dye possesses carcinogenic qualities and may induce health issues, including ocular irritation, dyspnea, gastrointestinal disturbances, dermal irritation, and systemic toxicity [6, 7]. Consequently, it is crucial to determine the appropriate method for treating waste containing this dye before its environmental discharge.

Several techniques, such as adsorption [8], membrane filtration [9], chemical oxidation [10], and coagulation-flocculation [11], have been employed to lower the Methylene blue dye concentration. Many of the employed processes generate by-products, rendering them inefficient [12]. Utilizing highly reactive hydroxyl radicals (•OH), Advanced Oxidation Processes (AOP) enable the mineralization of practically all organic molecules into CO_2, H_2O, and harm-less compounds [13]. One notable AOP technology is the utilization of photocatalysts derived from semiconductor materials. This approach offers cost-effectiveness and a rapid degradation process [14]. A range of semiconductors has been utilized for the photocatalytic degradation of Methylene blue dye, including CuO [2], MnO_2 [15], TiO_2 [16], NiO [17], and Nb/MCM-41 [18].

NiO serves as a p-type semiconductor frequently employed in photocatalytic degradation processes. Nevertheless, the utilization of NiO is marked by a considerable rate of electron-hole recombination. The rapid recombination of electrons and holes may lead to a decrease in a reduction of free radical generation, consequently diminishing the efficiency of the photocatalytic process. Furthermore, NiO possesses an expansive band gap energy of 3.6 to 4.0 eV, allowing it to essentially absorb ultraviolet light [19, 20]. Enhancing the efficiency of NiO as a catalyst can be achieved through the modification of various materials. Numerous investigations have explored modifications of NiO, including Co_3O_4/NiO [21], ZnO/La_2O_3/NiO [22], and NiO/$NiFe_2O_4$ [23].

Bentonite is a naturally abundant mineral that is very inexpensive and readily accessible. Bentonite is non-toxic and environmentally friendly, ensuring its application in catalytic reactions does not generate residues. Bentonite exhibits a layered structure with an extensive surface area, making it highly effective as a catalyst support [24].

The modification of NiO using bentonite/Fe_3O_4 in enhanced catalysts that exhibit magnetic properties, robust photocatalytic activity, stability, and effectiveness in acidic environments, as well as efficiency in harnessing visible light [23]. Fe_3O_4 represents a category of ferrite compounds

characterized by their environmental friendliness, thermomechanical stability, notable magnetic properties, and facilitating separation from the liquid medium when subjected to an external magnetic field [25, 26].

This research focused on the synthesis of a bentonite/Fe_3O_4@NiO composite employed for Methylene blue dye degradation with the help of visible light. The observed variables included catalyst dose, concentration, pH solution, and contact time. In addition, the evaluation of reaction kinetics and the reusability of the bentonite/Fe_3O_4@NiO composite were undertaken.

II. Materials and Methods

A. Materials

The materials utilized comprise $FeCl_2 \cdot 4H_2O$, $FeCl_3 \cdot 6H_2O$, NaOH, $Ni(NO_3)_2 \cdot 6H_2O$, HCl, and Methylene blue dye in analytical quality and utilized without further purification sourced from Merck, Germany. Bentonite is sourced from Sarolangun Regency, located in Jambi Province, Indonesia.

B. Synthesis of Bentonite/Fe_3O_4

Bentonite/Fe_3O_4 was produced in a mass ratio of 2:1. Total of 1.72 g of $FeCl_2 \cdot 4H_2O$, 4.66 g of $FeCl_3 \cdot 6H_2O$, and 4.0 g of bentonite were dissolved in 25 mL of distilled water. The mixture was stirred at a speed of 120 rpm, accompanied by the flow of N_2 gas, and maintained at a temperature of 60 °C [27]. A 2 M NaOH solution was incrementally added until the pH of the solution reached around 10 over 90 minutes, forming a black precipitate. Bentonite/Fe_3O_4 was extracted from the solution and rinsed with distilled water until achieving a neutral pH and subsequently subjected to drying in an oven at a temperature of 80 °C for 2 h.

C. Synthesis of Bentonite/Fe_3O_4@NiO Composite

$Ni(NO_3)_2 \cdot 6H_2O$, as much as 3.89 g, was dissolved in 25 mL of distilled water. 1 g of bentonite/Fe_3O_4 was added to the solution. The mixture was stirred at a speed of 120 rpm while adding 2 M NaOH solution gradually until the pH was ± 10. The precipitate was washed with distilled water until the pH was neutral. Furthermore, the precipitate was dried at a temperature of 80 °C for 2 h. Finally, the resulting powder was calcined at 250 °C for 3 h [28].

D. Characterizations Methods

The crystal phase of the composite was assessed using X-ray diffraction (PANalytical XRD) with Cu kα radiation (λ = 1.540598 Å and θ = 10–100°) at room temperature. A scanning electron microscope with energy-dispersive X-ray capabilities (SEM-EDX JEOL JSM-6510LA) was employed to examine the morphology and elemental composition. The absorbance and band gap energy were determined using UV-vis Diffuse Reflectance Spectroscopy (UV-DRS Hitachi U-2900). The magnetic properties of the material were examined employing a Vibrating Sample Magnetometer (VSM Oxford Type 1.2 T). Dye absorbance analysis was conducted using Thermo Orion AquaMate 8000 [AQ8000] UV-Vis Spectrophotometer.

E. pHpzc

The pHpzc was determined following this procedure. Multiple Erlenmeyer flasks containing 0.15 g of bentonite/Fe_3O_4@NiO composite were introduced with 50 mL of 0.01 M NaCl. A combination of 0.1 M NaOH and 0.1 M HCl was used to adjust the initial pH value of the solution to a range of 2–12. The mixture was then stirred at 100 rpm for 48 h at ambient temperature. The pHpzc value represents the junction of the initial pH and ΔpH.

F. Photocatalytic degradation of Methylene blue dye

The procedure was conducted using the batch method. 50 mg of the bentonite/Fe_3O_4@NiO composite was distributed to 100 mL of a 20 mg/L Methylene blue dye solution in a 250 mL container. To reach equilibrium, the mixture was stirred in a dark room for 25 min. After that, it was exposed to visible light (a halogen lamp with a 500 W bulb and a wavelength of 450 nm). The radiation source is approximately 15 cm from the dye. Degradation factors encompass the amount of catalyst (0.025–0.1 g), initial dye concentration (20–80 mg/L), and solution pH (4–10), with a volume of Methylene blue dye 100 mL and an irradiation time ranging from 25 to 125 min. After the degradation process, the catalyst is separated from the solution using an external magnet. The degradation of dye is quantified as Ct/Co, where Ct represents the residual dye concentration and Co denotes the initial concentration of Methylene blue dye.

III. Result and Discussion

A. Characterization of Bentonite, Bentonite/Fe_3O_4, and Bentonite/Fe_3O_4@NiO composite

The structure and phase characteristics of Fe_3O_4, bentonite/Fe_3O_4, and bentonite/Fe_3O_4@NiO composites are all revealed by XRD examination. Bentonite is a clay mineral consisting mostly of montmorillonite. The XRD pattern reveals a distinct peak at 2θ = 26.6°, signifying the presence of SiO_2, as presented in Fig. 1(a). Fig. 1(b) displays peaks at 2θ = 30.1, 35.4, 43.1, 53.4, 57.0, and 62.5°, corresponding to the (220), (311), (400), (442), (511), and (440) crystal planes of the inverse spinel cubic Fe_3O_4 structure (JCPDS No. 65-3107) [29].

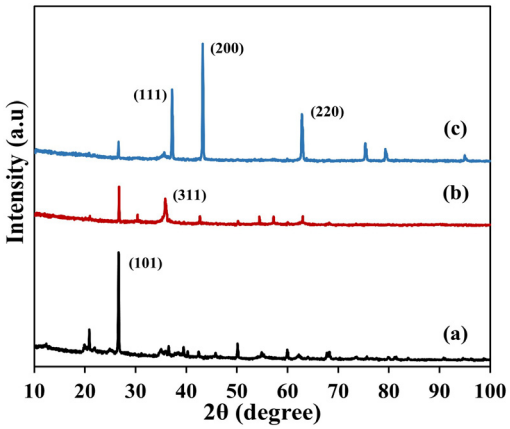

Fig. 1. Characterization of X-ray diffraction of (a) bentonite, (b) bentonite/Fe_3O_4, and (c) bentonite/Fe_3O_4@NiO composite.

The incorporation of NiO in the bentonite/Fe_3O_4@NiO composite is evidenced by the distinct and narrow peaks at angles 2θ = 37.2, 43.3, and 62.9°, corresponding to the crystal planes (111), (200), and (220) illustrated in Fig. 1(c). These peaks align with JCPDS data No. 47–1049 [19]. The existence of peaks for each element in the composite signifies

the incorporation of Fe_3O_4, NiO, and bentonite.

Fig. 2 demonstrates the magnetic characteristics of Fe_3O_4, bentonite/Fe_3O_4 and bentonite/Fe_3O_4@NiO. The saturation magnetization values for the three materials are 75.66, 61.07, and 51.02 emu/g, respectively. The saturation magnetization value of Fe_3O_4 is higher than that of other studies using the same method, namely 72 emu/g [30]. The magnetic characteristics of the material diminish as the proportion of bentonite (a non-magnetic substance) in the composite [27]. Although the bentonite/Fe_3O_4@NiO composite exhibits the least magnetic properties, it is still significantly affected by magnetic fields.

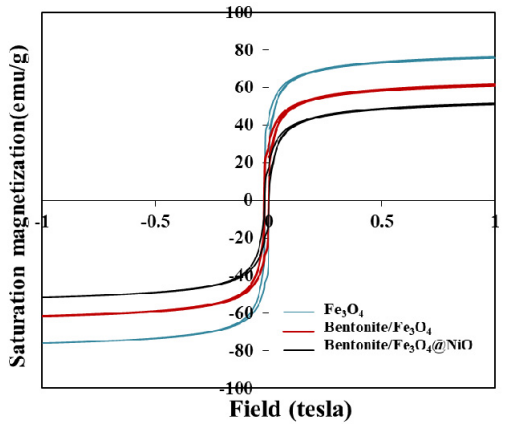

Fig. 2. Assessment of magnetic saturation of Fe_3O_4, bentonite/Fe_3O_4, and bentonite/Fe_3O_4@NiO composite.

The wavelength and band gap analysis employing UV-visible spectroscopy is shown in Fig. 3. The wavelength was measured between 200-900 nm, revealing that the absorption peak of bentonite/Fe_3O_4@NiO composites occurs at 340 nm, 455 nm, and 600 nm. It signifies that the composite absorbs not just in the ultraviolet and visible spectra. Absorption at 340 nm indicates the presence of NiO in the composite. NiO generally absorbs light in the ultraviolet spectrum, specifically between 300 and 400 nm, associated with the d-d transition [31, 32]. The energy band gap was ascertained utilizing the Tauc equation (1) as follows:

$$\alpha h\nu = A\,(h\nu - Eg)^n \quad (1)$$

where α is the absorption coefficient, h is Planck's constant, ν is the frequency of light, and Eg indicates the value of the band. The band gap of NiO is 3.72 eV, exceeding that of bentonite/Fe_3O_4@NiO and bentonite/Fe_3O_4 composites, which are 1.96 eV and 1.82 eV, respectively. Integration of bentonite, Fe_3O_4, and NiO decreases the band gap of NiO. A p/n-type heterojunction is established in bentonite/Fe_3O_4@NiO composites. This interaction enables the efficient transport of cargo and reduces the minimum energy necessary for electron excitation, thereby reducing the optical band gap [33].

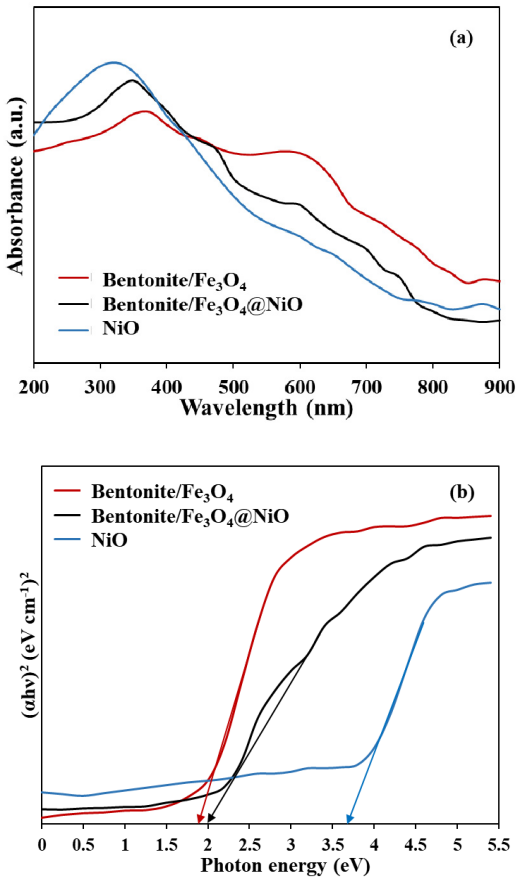

Fig. 3. (a) Wavelength (b) Band energy gap of bentonite/Fe_3O_4, bentonite/Fe_3O_4@NiO composite and NiO.

Fig. 4 illustrates the morphology of bentonite, bentonite/Fe_3O_4, and bentonite/Fe_3O_4@NiO composites. The bentonite structure exhibits typical layered properties (interlayer) with overlapping layers. Fe_3O_4 is situated within the layers or on the surface of bentonite. Simultaneously, NiO is dispersed over the surface of bentonite/Fe_3O_4.

EDX analysis results validated the successful synthesis, evidenced by the presence of Ni components in the bentonite/Fe_3O_4 composites, as presented in Fig. 5 and Table 1. Bentonite comprises three primary elements: O, Al, and Si. Additionally, there was an augmentation in the proportion of Fe elements in bentonite/Fe_3O_4 and Ni in the bentonite/Fe_3O_4@NiO composites.

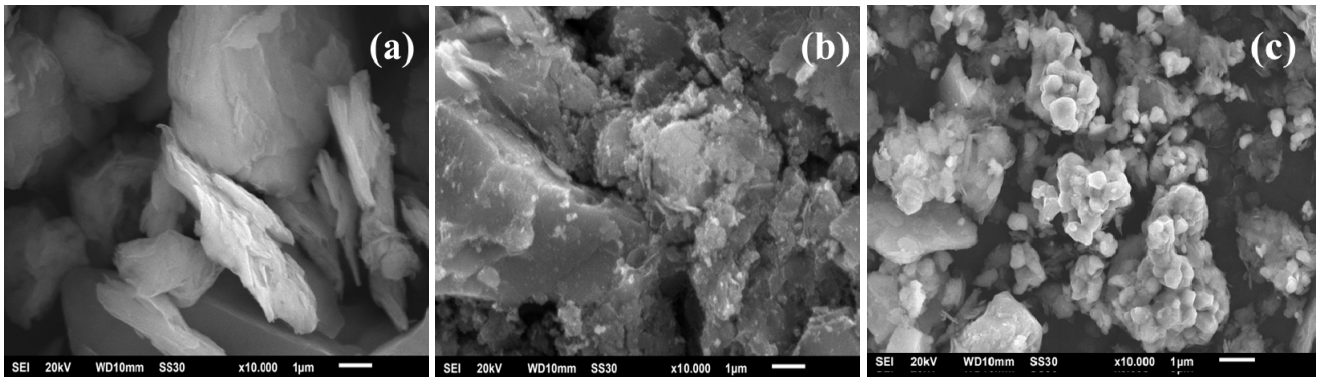

Fig. 4. Secondary electron image of (a) bentonite, (b) bentonite/Fe_3O_4, and (c) bentonite/Fe_3O_4@NiO composite.

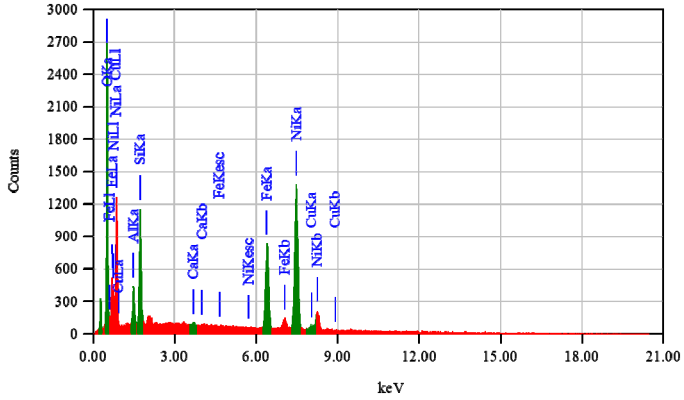

Fig. 5. EDX spectra of bentonite/Fe_3O_4@NiO composite.

Table 1. Elemental composition of EDX analysis

Elements	Mass (%)		
	Bentonite	Bentonite/Fe_3O_4	Bentonite/Fe_3O_4@NiO
O	59.85	51.95	48.57
Al	8.64	5.88	3.48
Si	27.78	12.94	9.59
K	0.47	0.32	0.16
Fe	1.22	28.34	21.13
Cu	1.00	0.28	0.39
Ca	0.36	0.11	0.09
Na	0.68	0.18	-
Ni			16.59

B. Evaluation of Photocatalytic Activity

Fig. 6 illustrates the pHpzc of the bentonite/Fe_3O_4@NiO composite. pHpzc is the pH value at which the charges on the material's surface are balanced, which is essential for optimum degradation conditions. The pHpzc of bentonite/Fe_3O_4@NiO composite in this investigation was 6.84. If the pH of the solution is less than or equal to pHpzc, the composite surface is positive, while it is negative when the pH of the solution is greater than or equal to pHpzc [34].

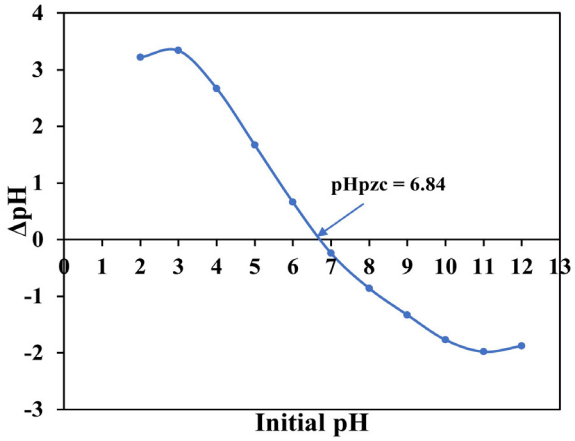

Fig. 6. pHpzc of Bentonite/Fe_3O_4@NiO composite.

The catalyst was added at an amount of 0.025, 0.05, 0.075, and 0.1 g into 100 mL of Methylene blue dye with a concentration of 20 mg/L. The degradation (Ct/C_o) increased from 0.025 to 0.05 g, as seen in Fig. 7(a). The increased availability of active sites due to a higher catalyst dosage facilitates the concurrent degradation of additional target molecules [35]. However, at 0.075 g, degradation diminishes; catalyst particles may induce aggregation and precipitation, consequently decreasing the effective surface area of the catalyst accessible for interaction with dye molecules [34].

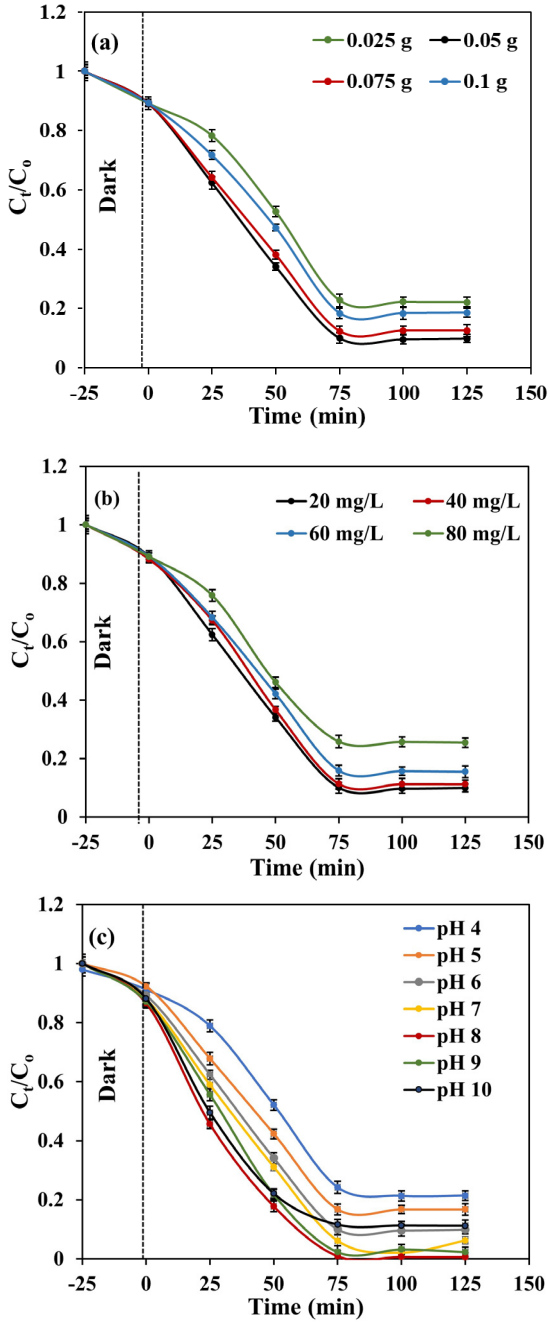

Fig. 7 (a) The impact of (b) amount of catalyst, (b) initial concentration, and (c) pH solution for Methylene blue dye degradation.

The impact of concentration was examined using a catalyst of 0.05 g and Methylene blue dye concentrations of 20, 40, 60, and 80 mg/L. The lowest C_t/C_o value indicating the optimum degrading efficiency occurs at 20 mg/L. The efficiency of degradation diminished as the concentration of Methylene blue dye increased (Fig. 7b). Increased dye concentrations resulted in an elevated number of dye molecules obstructing the radiation light essential for activating the catalyst. As a result, the intensity of light reaching the catalyst surface decreases, so the number of electrons and holes produced by the catalyst for degradation also decreases. In addition, the catalyst surface may be covered by an increasing number of dye molecules, some of which are adsorbed on the catalyst surface, thereby reducing the amount of active surface area available for degradation. This limits the direct interaction between the dye molecules and the free radicals generated by the catalyst [36, 37].

The pH influences the surface charge of the catalyst, the stability of the dye, and the generation of radicals. Consequently, it is crucial to evaluate the impact of pH. This investigation investigated the effect of pH using a 20 mg/L concentration of Methylene blue dye, amount of catalyst 0.05 g, and a pH range of 4–10. Fig. 7(c) indicates that the optimal pH for photocatalytic degradation is 8, achieving an efficiency of 99.35%. Methylene blue dye typically degrades photocatalytically in alkaline conditions [38, 39]. Bentonite/Fe_3O_4@NiO composite possesses a pHpzc of 6.80, whereas Methylene blue dye is a cationic dye; at a solution pH below the pHpzc, repulsion occurs between the catalyst and the dye. At alkaline conditions, the catalyst is negatively charged while the Methylene blue dye is positively charged so that an electrostatic attraction occurs. The efficiency of the photodegradation process increases with a higher concentration of Methylene blue dye near the active surface. A significant quantity of hydroxyl radicals is generated at pH 8, hence enhancing the efficiency of the breakdown process. Elevated pH levels increase the presence of OH^- ions, which compete with hydroxyl radicals during the degradation process. The possible degradation mechanism of Methylene blue dye by the Bentonite/Fe_3O_4/NiO composite entails a producing radical such as superoxide ($\bullet O_2^-$) and hydroxyl radicals (•OH) that decompose dye molecules into simpler compounds [40].

$$\text{Bentonite/}Fe_3O_4\text{@NiO} + h\nu \rightarrow e_{CB}^- + h_{VB}^+ \quad (2)$$

$$e_{CB}^- + O_2 \rightarrow \bullet O_2^- \quad (3)$$

$$h_{VB}^+ + H_2O \rightarrow \bullet OH + H^+ \quad (4)$$

$$\text{Dye} + \bullet OH + \bullet O_2^- \rightarrow CO_2 + H_2O + \text{other product} \quad (5)$$

C. Kinetics Study

The examination of Methylene blue dye degradation kinetics is crucial for elucidating the reaction rate and processes underlying the degradation process. The kinetics of photocatalytic degradation of the bentonite/Fe_3O_4@NiO composite for Methylene blue dye under visible light was assessed by plotting the logarithmic ratio of the initial concentration to the dye concentration at various reaction times. The kinetic study followed pseudo-first-order reaction kinetics, as outlined by the Langmuir-Hinshelwood model. The pseudo-first-order equation is defined in the following Eq. [6]:

$$\ln C/C_0 = -kt \quad (6)$$

where C and C_0 (mg/L) represent the initial concentration of Methylene blue dye each time (t), and k is the kinetic constant. The kinetic investigations were carried out during a 10–70 min period using a 20 mg/L concentration of Methylene blue dye, an amount of catalyst of 0.05, and a pH of 8 solution. Based on the coefficient of determination value obtained (R^2) of 0.9945, it indicates the suitability of the data with pseudo-first-order (Fig. 8). The k value obtained from the slope is 0.0665 min^{-1}. The kinetics of Methylene blue dye degradation from other studies using CuO, ZnO/La_2O_3/NiO, and chitosan/NiO showed the same results, namely following pseudo-first-order with k values of 0.000681, 0.0621, and 0.00138 min^{-1} [2, 21, 36]. The k value of the results of this investigation is greater than that of the studies.

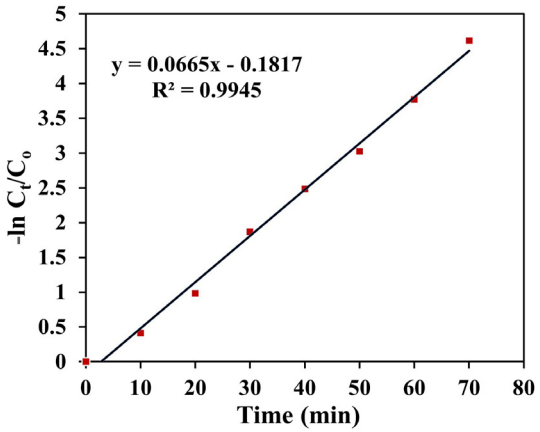

Fig. 8. Pseudo-first-order kinetics for the degradation of Methylene blue dye using bentonite/Fe_3O_4@NiO composite.

D. Reusability Study

Another crucial part of photocatalysis is conducting reusability research to ensure stability and continued degradation of Methylene blue dye. The catalyst's reusability decreases operational expenses. Following the catalyst's removal from the solution with a magnet, it was washed with acetone and deionized water. Subsequently, it was left to dry at 80°C for three hours. Reusability was conducted during five successive cycles, as illustrated in Fig. 9.

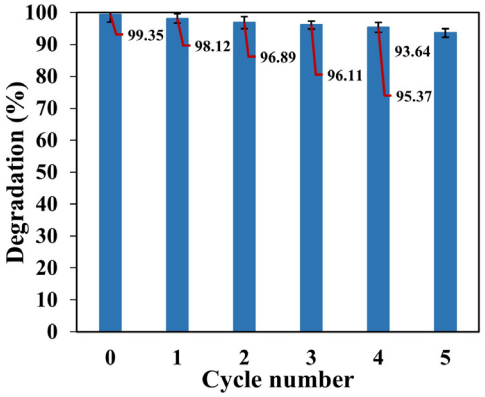

Fig. 9. Reusability of bentonite/Fe_3O_4@NiO composite for Methylene blue dye degradation.

The catalyst exhibited commendable performance across five cycles, with degradation rates of 98.12%, 96.89%, 96.11%, 95.37%, and 93.64%, respectively. During deterioration, the reaction products may adhere to the composite surface, obstructing access to the active areas. This results in a reduction in the surface area accessible for subsequent reactions, hence diminishing the catalyst's activity [41]. In addition, leaching from the catalyst structure into the solution also contributes to the decreased efficiency due to the decreased number of active components involved in the photocatalysis process [42, 43]. The reduction in degradation efficiency in this study was 5.71%, significantly lower than in previous investigations, such as the one where the $CeVO_4$/bentonite catalyst used for Methylene blue dye recycling exhibited a decline from 99% to 74.78% after five cycles [44].

E. FTIR Analysis

The analysis of FTIR was utilized to elucidate the alterations in the catalyst structure prior to and following

degradation. The study was conducted within the wave number range of 4000 to 400 cm^{-1} (Fig. 10). It appears that the bentonite/Fe_3O_4@NiO composite, both prior to and subsequent to its application in the photocatalytic degradation of Methylene blue dye, did not exhibit any alterations in wave number. This signifies the catalyst has considerable chemical stability. The broad peaks at wave numbers around 3200-3600 cm^{-1} and 1630 cm^{-1} correspond to O-H bonds resulting from the absorption of water molecules or hydroxyl group bonds on the bentonite surface with metal oxides (M-OH) [45]. Bentonite exhibits two distinct peaks at 532 cm^{-1} and 466 cm^{-1}, which are indicative of Al-O-Si stretching vibrations and Si-O-Si vibrations, respectively [46]. These peaks coincide with the Fe-O peak of Fe_3O_4 [47]. The wave number of 1031 cm^{-1} corresponds to the Si–O stretching vibration of silica tetrahedra within the bentonite structure. The NiO band is situated within the 400–600 cm^{-1} range, reflecting the distinctive vibration of the Ni–O bond.

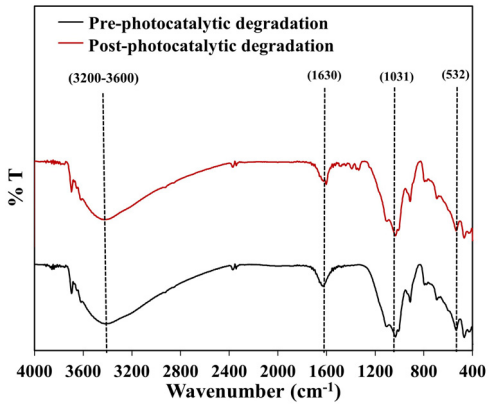

Fig. 10. FTIR spectra of bentonite/Fe_3O_4@NiO composite.

IV. Conclusion

The present study effectively synthesized a bentonite/Fe_3O_4@NiO composite and utilized it for the degradation of Methylene blue dye. This composite exhibits magnetic properties and possesses a low band gap. The catalyst demonstrated significant degradation capacity under visible light irradiation, achieving optimal conditions with a Methylene blue dye concentration of 20 mg/L, an amount of catalyst 0.05 g, a pH of 8, and an irradiation time of 75 minutes, resulting in a degradation rate of 99.35% for Methylene blue dye. This catalyst demonstrated significant stability, with a degradation efficiency of 93.64% after five cycles of reuse. The findings suggest a potential approach for addressing water contamination caused by dyes.

Conflict of Interest

The authors declare no conflict of interest.

Author Contributions

F.R.: Data collection and laboratory data processing, H.: Methodology and writing, A.R.: Supervision and editing, M.: Review and editing, E.I.: Data analysis and P.L.H.: Conceptualization of ideas and experimental design.

Acknowledgment

This research was facilitated by a grant from the Hibah Profesi Program, awarded by the DIPA of the Public Service Agency of Universitas Sriwijaya on November 24, 2024 (SP DIPA-023.17.2.677515/2024).

References

[1] S. Mallick, D. Barik, and N. Pradhan, "*Commelina erecta*, L. biomass-silver nanoparticle composite as a heterogeneous catalyst for methylene blue degradation," *Applied Catalysis O: Open*, vol. 192, pp. 1–10, 2024.

[2] A. Ahmad, A.N. Siyal, A. Elci, and N. H. Kalwar, "*Ziziphus nummularia* leaves extract mediated CuO nanostructures for photocatalytic degradation of Methylene blue," *Desalination and Water Treatment*, vol. 320, pp. 1–6, 2024.

[3] L. Mouni, L. Belkhiri, J. Bolliger, A. A. Bouzaza, A. Assadi, A. Tirri, F. Dahmoune, K. Madani, and H. Remini, "Removal of Methylene blue from aqueous solutions by adsorption on kaolin: Kinetic and equilibrium studies," *Applied Clay Science*, vol. 153, pp. 38–45, 2018.

[4] M. A. Hossain, M. M. H. Mondol, and S. H. Jhung, "Functionalized metal-organic frame-work-derived carbon: Effective adsorbent to eliminate Methylene blue, a small cationic dye from water," *Chemosphere*, vol. 303, pp. 1–8, 2022.

[5] R. S. Shinde, V. A. Adole, S. D. Khairnar, P. B. Koli, and T. B. Pawar, "Study of Fe_3O_4 and Cu^{2+} doped modified Fe_3O_4 nano catalyst for photocatalytic degradation of methylene blue and eriochrome black-T dyes: Synthesis, characterization, and antimicrobial assessment," *Inorganic Chemistry Communication*, vol. 170, pp. 1–20, 2024.

[6] H. Karimi, M. A. Heidari, H. B. M. Emrooz, and M. Shokouhimehr, "Carbonization temperature effects on adsorption performance of metalorganic framework derived nanoporous carbon for removal of Methylene blue from wastewater; experimental and spectrometry study," *Diamond and Related Materials*, vol. 108, pp. 1–14, 2020.

[7] M. A. Ali and I. M. Maafa, "Recent literature review of cerium-containing photocatalysts used for methylene blue degradation," *Journal of Hazardous Materials Advances*, vol. 16, pp. 1–26, 2024.

[8] Y. Bian, X. Song, Y. Han, G. Wang, and H. Qiao, "Carboxyl functionalized covalent organic framework material for selective adsorption of methylene blue in aqueous solutions," *Tetrahedron Letters*, vol. 150, pp. 1–8, 2024.

[9] E. W. Trisnawati, V. Suryanti, and E. Pramono, "Fabrication and evaluation of PVDF membranes modified with cellulose and cellulose esters from peanut (*Arachis hypogea* L.) shell for application in Methylene blue filtration," *JCIS Open*, vol. 16, pp. 1–8, 2024.

[10] M. A. V. Garrido, M. C. Portillo, H. Juarez, A. Luna, and L. E. S. Rosa, "Low cost chemical bath deposition synthesis of zinc oxide/zinc sulfide composite and zinc hydrozincite for Methylene blue degradation," *Inorganic Chemistry Communications*, vol. 164, pp. 1–9, 2024.

[11] S. Ihaddaden, D. Aberkane, A. Boukerroui, and D. Robert, "Removal of Methylene blue (basic dye) by coagulation-flocculation with biomaterials (bentonite and *Opuntia ficus* indica)," *Journal of Water Process Engineering*, vol. 49, pp. 1–12, 2022.

[12] S. Sankaranarayanan, S. Subramanian, S. Hussain, and G. K. Mamidipudi, "Hierarchical nanostructures of MoS_2 for visible light photocatalytic degradation of Methylene blue dye," *Physica B: Condensed Matter*, vol. 692, pp. 1–12, 2024.

[13] E. Arulkumar, and S. Thanikaikarasan, "Structure, morphology, composition, optical properties and catalytic activity of nanomaterials CuO, NiO, CuO/NiO using Methylene blue," *Optik (Stuttgart)*, vol. 302, pp. 1–22, 2024.

[14] S. Subramanian, S. Ganapathy, and S. Subramanian, "Superior photocatalytic activities of p-CdTe QDs/n-$NiTiO_3$ NFs system for the treatment of hazardous dye industrial effluents," *Journal of Environmental Chemical Engineering*, vol. 10, pp. 106941–106951, 2022.

[15] A. S. Belousov, E. V. Suleimanov, A. A. Parkha-cheva, D. G. Fukina, A. V. Koryagin, A. V. Koroleva, E. V. Zhizhin, and A. P. Gorshkov, "Regulating of MnO_2 photocatalytic activity in degradation of organic dyes by polymorphic engineering," *Solid State Sciences*, vol. 132, pp. 1–14, 2022.

[16] A. Ribeiro, H. M. Souza, F. S. Rodembusch, T. B. Wermuth, O. R. K. Montedo, R. Moreno, J. Venturini, and S. Arcaro, "Nitrogen assisted one-step hydrothermal synthesis of commercial TiO_2 for Methylene blue degradation under visible light irradiation," *Ceramics International*, vol. 50, pp. 34240–34250, 2024.

[17] G. Jayakumar, A. A. Irudayaraj, A. D. Raj, "Photocatalytic degradation of methylene blue by nickel oxide nanoparticles," *Materials Today: Proceedings*, vol. 4, pp. 11690–11695, 2017.

[18] C. D. Gomez, and J. E. Rodriguez-Paez, "Photocatalytic properties of Nb/MCM-41 molecular sieves: Effect of the synthesis conditions," *Coating*, vol. 5, no. 3, pp. 511–526, 2015.
[19] K. V. Chandekar, B. Palanivel, F. H. Alkallas, A. B. G. Trabelsi, A. Khan, I. M. Ashraf, S. AlFaify, and M. Shkir, "Photocatalytic activities of Mg doped NiO NPs for degradation of Methylene blue dye for harmful contaminants: A kinetics, mechanism and recyclability," *Journal of Physics and Chemistry of Solids*, vol.178, pp. 1–14, 2023.
[20] V. Kavinkumar, D. P. Jaihindh, A. Verma, K. Jothivenkatachalam, and Y.P. Fu, "Influence of cobalt substitution on the crystal structure, band edges and photocatalytic properties of hierarchical Bi_2WO_6 microspheres," *New Journal of Chemistry*, vol. 43, pp. 9170–9182, 2019.
[21] M. Zeba, Z. Anjum, S. Mumtaz, M. Khalid, and M. Hafeez, "*Jasminum mesyni* mediated synthesis of Co_3O_4/NiO nanocomposite for methylene blue degradation," *Desalination and Water Treatment*, vol. 317, pp. 1–6, 2024.
[22] J. P. Shubha, N. V. Sushma, S. F. Adil, M. Khan, M. E. Assal, M. R. Hatshan, and B. Shaik, "ZnO/La_2O_3/NiO based ternary heterostructure nano-photocatalyst: Preparation, characterization and its application for the degradation of Methylene blue," *Journal of King Saud University – Science*, vol. 34, pp. 1–9, 2022.
[23] P. L. Hariani, M. Said, A. Rachmat, A Nurmansyah, and Ra. H. T. Amallia, "Comparison of the photocatalytic degradation of Congo red dye using NiO and NiO-$NiFe_2O_4$ composite," *International Journal of Environmental Science and Development*, vol. 13, no. 3, pp. 57–62, 2022.
[24] S. M. Rahimi, A. H. Panahi, N. S. M. Moghaddam, E. Allahyari, and N. Nasseh, "Breaking down of low-biodegradation Acid Red 206 dye using bentonite/Fe_3O_4/ZnO magnetic nanocomposite as a novel photo-catalyst in presence of UV light," *Chemical Physics Letters*, vol. pp. 1–11, 2022.
[25] L. Zhang, X. Liu, M. Zhang, H. Yuan, L. Zhang, and J. Lu, "Facile construction of dual functional Fe_3O_4@C-MoO_2-Ni composites for catalysis and adsorption," *Applied Surface Science*, vol. 494, pp. 783–794, 2019.
[26] S. Liu, B. Yu, S. Wang, Y. Shen, and H. Cong, "Preparation, surface functionalization and application of Fe_3O_4 magnetic nanoparticles," *Advances in Colloid and Interface Science*," vol. 281, pp. 1–30, 2020.
[27] F. Riyanti, H. Hasanudin, A. Rachmat, W. Purwaningrum, and P. L. Hariani, "Photocatalytic degradation of Methylene blue and Congo red dyes from aqueous solutions by bentonite-Fe_3O_4 magnetic," *Communications in Science and Technology*, vol. 8, no. 1, pp. 1–9, 2023.
[28] P. Koohi, A. Rahbar-kelishami, and H. Shayesteh, "Efficient removal of congo red dye using Fe_3O_4/NiO nanocomposite: Synthesis and characterization," *Environmental Technology & Innovation*, vol. 23, pp. 1–13, 2021.
[29] S. Chkirida, N. Zari, R. Achour, H. Hassoune, A. Lachehab, A. K. Qaiss, and R. Bouhfid, "Highly synergic adsorption/photocatalytic efficiency of alginate/bentonite impregnated TiO_2 beads for wastewater treatment," *Journal of Photochemistry and Photobiology A: Chemistry*, vol. 412, pp. 1–11, 2021.
[30] T. Li, T. Yang, Z. Yu, G. Xu, M. Du, Y. Guan, and C. Guo, "An innovative magnetic bar separator for removal of chromium ions in tanning wastewater," *Journal of Water Process Engineering*, vol. 40, pp. 1–8, 2021.
[31] K. Maniammal, G. Madhu, and V. Biju, "Nanostructured mesoporous NiO as an efficient photo-catalyst for degradation of Methylene blue: Structure, properties and performance," *Nano-Structures & Nano-Objects*, vol. 16, pp. 266–275, 2018.
[32] M. El-Kemary, N. Nagy, and I. El-Mehasse, "Nickel oxide nanoparticles: Synthesis and spectral studies of interactions with glucose," *Materials Science in Semiconductor Processing*, vol. 16, pp. 1747–1752, 2013.
[33] S. Raha, M. Ahmaruzzaman, "Enhanced performance of a novel superparamagnetic g-C_3N_4/NiO/ZnO/Fe_3O_4 nanohybrid photocatalyst for removal of esomeprazole: Effects of reaction parameters, co-existing substances and water matrices," *Chemical Engineering Journal*, vol. 395, pp. 1–23, 2020.
[34] F. Golrizkhatami, L. Taghavi, N. Nasseh, and H.A. Panahi, "Synthesis of novel $MnFe_2O_4$/BiOI green nanocomposite and its application to photo-catalytic degradation of tetracycline hydrochloride: (LC-MS analyses, mechanism, reusability, kinetic, radical agents, mineralization, process capability, and purification of actual pharmaceutical wastewater," *Journal of Photochemistry and Photobiology A: Chemistry*, vol. 444, pp. 1–16, 2023.
[35] N. P. Moraes, F. N. Silva, M. L. C. P. Silva, T. M. B. Campas, and G. P. Thim, L. A, "Rodrigues.Methylene blue photodegradation employing hexagonal prism-shaped niobium oxide as heterogeneous catalyst: Effect of catalyst dosage, dye concentration, and radiation source," *Materials Chemistry and Physics*, vol. 214, pp. 95–106, 2018.
[36] C. Xu, G. P. Rangailah, and X. S. Zhao, "Photocatalytic degradation of Methylene blue by titanium dioxide: Experimental and modeling study," *Industrial & Engineering Chemistry Research*, vol. 53, pp. 14641–14649, 2014.
[37] M. H. El-Newehy, A. Aldalbahi, B. M. Thamer, and M. M. Abdulhameed, "Photocatalytic degradation of methylene blue using chitosan/NiO nanocomposite: A comprehensive exploration," *Optical Materials Express*, vol. 152, pp. 1–9, 2024.
[38] M. Moztahida, and D. S. Lee, "Photocatalytic degradation of Methylene blue with P_{25}/graphene/polyacrylamide hydrogels: Optimization using response surface methodology," *Journal of Hazardous Materials*, vol. 400, pp. 1–11, 2020.
[39] A. Boucherdoud, D. E. Kherroub, K. Dahmani, O. Douinat, A. Seghier, B. Bestani, and N. Bender-douche, "Polyaniline/cupric oxide organometallic nanocomposites as a sonocatalyst for the degradation of methylene blue: Experimental study, RSM optimization, and DFT analysis," *Journal of Organometallic Chemistry*, vol. 1022, pp. 1–14, 2024.
[40] D. Rostamzadeh, and S. Sadeghi, "Ni doped zinc ox-ide nanoparticles supported bentonite clay for photocatalytic degradation of anionic and cationic synthetic dyes in water treatment," *Journal of Photochemistry and Photobiology A: Chemistry*, vol. 431, pp. 1–14, 2022.
[41] K. G. N. Quiton, M. C. Lu, and Y. H. Huang, "Synergistic degradation of Methylene blue by novel Fe-Co bimetallic catalyst supported on waste silica in photo-Fenton-like system," *Sustainable Environment Research*, vol. 32, pp. 1–18, 2022.
[42] B. A. Abdulkadir, R. S. R. M. Zaki, A. A. Jalil, J. F. Su, and H. D. Setiabudi, "Synergistic effects of Fe_2O_3 supported on dendritic fibrous SBA-15 for superior photocatalytic degradation of methylene blue," *Materials Science in Semiconductor Processing*, vol. 185, pp. 1–3, 2025.
[43] A. A. Ahmed, and S. Sumathi, "Facile synthesis of CuO/$CePO_4$ nanocomposite for the photocatalytic degradation of organic pollutants under visible light," *Inorganic Chemistry Communications*, vol. 161, pp. 1-12, 2024.
[44] H. Farhadi, M. Mousavi-Kamazani, N. Keramati, and S. Alamdari, One-step hydrothermal synthesis of $CeVO_4$/bentonite nanocomposite as a dual-functional photocatalytic adsorbent for the removal of methylene blue from aqueous solutions," *Scientific Reports*, vol. 14, pp. 1–13, 2024.
[45] L. Jiang, Q. Ye, J. Chen, Z. Chen, and Y. Gu, "Preparation of magnetically recoverable bentonite–Fe_3O_4–MnO_2 composite particles for Cd(II) removal from aqueous solutions," *Journal of Colloid and Interface Science*, vol. 513, pp. 748–759, 2018.
[46] J. Dai, X. Wei, Z. Cao, Z. Zhou, P. Yu, J. Pan, T. Zou, C. Li, and Y. Yan, "Highly-controllable imprinted polymer nanoshell at the surface of magnetic halloysite nanotubes for selective recognition and rapid adsorption of tetracycline," *RSC Advences*, vol. 4, pp. 7967–797, 2014.
[47] E. Yang, M. Cao, X. Ren, J. Jiang, Q. An, Z. Zhang, J. Gao, X. Yang, and D. Zhang, "Synthesis of Fe_3O_4 nanoparticles functionalized polyvinyl alcohol/chitosan magnetic composite hydrogel as an efficient adsorbent for chromium (VI) removal," *Journal of Physics and Chemistry of Solid*s, vol. 121, pp. 102–109, 2018.